

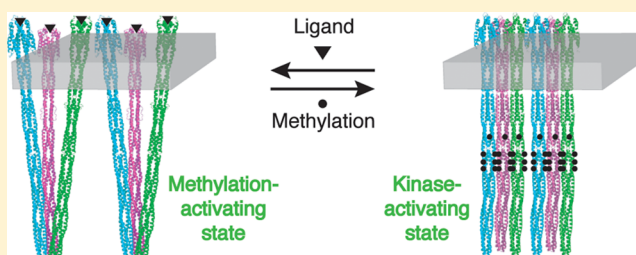
# Ligand Affinity and Kinase Activity Are Independent of Bacterial Chemotaxis Receptor Concentration: Insight into Signaling Mechanisms

Fe C. Sferdean,<sup>†</sup> Robert M. Weis,<sup>\*,†,‡</sup> and Lynmarie K. Thompson<sup>\*,†,‡</sup>

<sup>†</sup>Department of Chemistry, <sup>‡</sup>Molecular and Cellular Biology Graduate Program, University of Massachusetts, Amherst, Massachusetts 01003, United States

## S Supporting Information

**ABSTRACT:** Binding of attractant to bacterial chemotaxis receptors initiates a transmembrane signal that inhibits the kinase CheA bound ~300 Å distant at the other end of the receptor. Chemoreceptors form large clusters in many bacterial species, and the extent of clustering has been reported to vary with signaling state. To test whether ligand binding regulates kinase activity by modulating a clustering equilibrium, we measured the effects of two-dimensional receptor concentration on kinase activity in proteoliposomes containing the purified *Escherichia coli* serine receptor reconstituted into vesicles over a range of lipid:protein molar ratios. The  $IC_{50}$  of kinase inhibition was unchanged despite a 10-fold change in receptor concentration. Such a change in concentration would have produced a measurable shift in the  $IC_{50}$  if receptor clustering were involved in kinase regulation, based on a simple model in which the receptor oligomerization and ligand binding equilibria are coupled. These results indicate that the primary signal, ligand control of kinase activity, does not involve a change in receptor oligomerization state. In combination with previous work on cytoplasmic fragments assembled on vesicle surfaces [Besschetnova, T. Y., et al. (2008) *Proc. Natl. Acad. Sci. U.S.A.* 105, 12289–12294], this suggests that binding of ligand to chemotaxis receptors inhibits the kinase by inducing a conformational change that expands the membrane area occupied by the receptor cytoplasmic domain, without changing the number of associated receptors in the signaling complex.



Two-component signaling pathways, a signal transduction motif that is widespread in prokaryotes and found in some eukaryotes, involve the autophosphorylation of histidine kinases and phosphotransfer to aspartyl groups of response regulators.<sup>1</sup> Bacterial chemotaxis is a well-studied two-component signaling system that allows bacteria to sense chemical gradients and bias swimming toward higher attractant concentrations.<sup>2</sup> The methyl-accepting chemotaxis receptors that provide the sensory input for this system have been the focus of numerous investigations that seek to understand the mechanism of transmembrane signaling. An intriguing property of these receptors is the formation of large receptor clusters, typically at the poles of the cell.<sup>3</sup> These clusters are thought to be important for receptor cooperativity<sup>4</sup> and adaptation<sup>5</sup> to mediate the sensitivity, dynamic range, and integration of the chemotaxis signaling network.<sup>6–9</sup> Clustering may also play a role in receptor activation, as observed for the EGF receptor and other receptors that are activated by ligand-induced dimerization or oligomerization.<sup>10,11</sup> Chemoreceptor clustering has been reported to vary with signaling state, but the evidence has been inconsistent. These data raise the question of whether a clustering equilibrium plays a role in the primary signal, ligand regulation of chemoreceptor activation of the kinase CheA.

Four chemotaxis receptors in *Escherichia coli* share the overall structure and interaction sites shown in Figure 1.<sup>12</sup> The high-

abundance receptors Tar and Tsr detect aspartate and serine, respectively, and the low-abundance receptors Trg and Tap detect ribose/galactose and dipeptides, respectively. These chemoreceptors are transmembrane  $\alpha$ -helical homodimers, based on crystal and NMR structures of the periplasmic, HAMP, and cytoplasmic domains.<sup>13–15</sup> The membrane-distal tip of the cytoplasmic domain binds two proteins, the histidine kinase CheA and a scaffolding protein CheW. The central region of the receptor cytoplasmic domain contains four glutamate residues that are methylated and demethylated, which allows the receptor to adapt to an ongoing stimulus. Both the CheR methyltransferase and the CheB methylesterase that modify these adaptation sites have been shown to bind to the carboxy terminus of the high-abundance receptors.<sup>16,17</sup> Replacing Glu with Gln at the adaptation sites mimics the effects of receptor methylation,<sup>18</sup> and the wild-type receptor is genetically encoded in an intermediate adaptation state, with two Glu and two Gln residues (Gln residues are initially deamidated to Glu residues by CheB).

Although not shown in Figure 1 for the sake of simplicity, chemotaxis receptors are interconnected by CheA and CheW

Received: June 6, 2012

Revised: August 6, 2012

Published: August 7, 2012

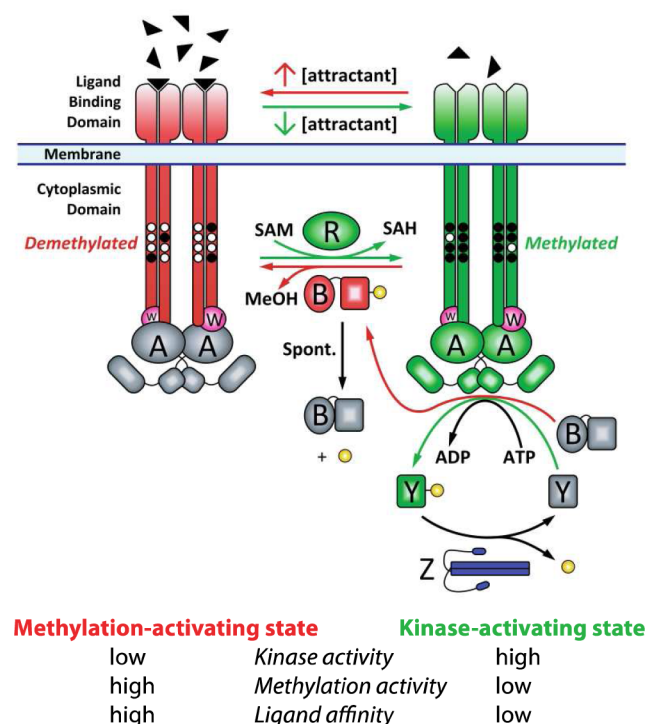


**Figure 1.** *E. coli* chemotaxis pathway depicted as a two-state signaling system. Receptor–CheW–CheA complexes are shown in kinase-stimulating (green, magenta, and green, respectively) and kinase-inhibiting (red, magenta, and gray, respectively) states. The binding of attractant (black triangles) inhibits the CheA kinase (gray A dimer) and stimulates the receptor methylation (black circles) via CheR (green R). Methylated receptors stimulate CheA (green A dimer). The two substrates of CheA, CheY (Y) and the methyltransferase (B), are activated by phosphorylation (yellow). CheY phosphate (green Y) propagates the tumble signal, and CheB phosphate (red B) provides negative feedback by demethylating (and deactivating) receptors. CheB dephosphorylates spontaneously. CheZ (blue Z dimer) dephosphorylates CheY phosphate. Two features not represented in the figure are the packing of receptor dimers into hexagonal arrays with CheA and CheW and the unknown receptor:CheA:CheW stoichiometry.

into hexagonal arrays that have been observed across a wide range of prokaryotes.<sup>19</sup> Furthermore, although the stoichiometry of the proteins in these arrays is not known, recent estimates suggest they contain more receptor than CheA and CheW: on the basis of measured stoichiometries of six Tsr's per CheA and CheW, it has been suggested that a pair of receptor trimer of dimers is needed to activate the dimeric CheA kinase.<sup>20</sup> Recent cryoelectron tomography studies have yielded models for the arrangement of receptor, CheA, and CheW in the signaling arrays.<sup>21,22</sup>

Receptor signaling is usually described in terms of a two-state equilibrium, with attractant occupancy and methylation shifting the equilibrium in opposite directions (Figure 1). In the absence of an attractant ligand, the receptor stimulates autophosphorylation of the histidine kinase CheA, which transfers the phosphate to either CheY or CheB. Phospho-CheY binds to the flagellar motor, causing a change from counterclockwise rotation of the flagellar bundle that propels the cell forward to clockwise rotation that disrupts the flagellar bundle and causes the cell to tumble. Phosphorylation also activates the CheB methyltransferase, which decreases the steady state level of receptor methylation that is determined by the

relative activities of CheR and CheB. Binding of an attractant ligand to the receptor turns off kinase activation and thus decreases levels of phospho-CheY and tumbling frequency, so that the cell makes longer runs in the presence of attractants such as Asp or Ser. Following this rapid change in tumbling frequency, adaptation occurs on a slower time scale: decreased levels of phospho-CheB lead to increased levels of receptor methylation, shifting the equilibrium back toward the kinase-activating state. The attractant-bound receptor is also more efficiently methylated by CheR, which contributes to the adaptation shift back to the kinase-activating state.

The focus of this study is to determine whether the extent of receptor clustering is different in the two signaling states depicted in Figure 1. We use the term cluster to refer to a receptor associated with other receptors, CheA, and CheW into an oligomeric multiprotein complex, with intermolecular contacts among the proteins within the cluster, as distinct from colocalized receptors that lack such contacts. Evidence from microscopy and in vivo cross-linking studies is mixed: some studies have reported that ligand binding decreases the level of receptor clustering or methylation increases the level of receptor clustering in cells. Libermann et al.<sup>23</sup> observed an increase in the degree of polar localization of CheA-containing complexes with methylation (Tar<sub>2Q2E</sub> ≈ half-methylated receptor relative to Tar<sub>4E</sub> = unmethylated adaptation state), using fluorescence microscopy of *E. coli* expressing CheA fused to YFP (yellow fluorescent protein). However, because these changes were much smaller than the measured changes in kinase activity, they concluded that changes in the assembly of CheA-containing clusters do not control the kinase.<sup>23</sup> On the basis of immunoelectron microscopy of *E. coli* cells expressing a single type of chemotaxis receptor, Lyberger et al.<sup>24</sup> reported that high-abundance receptors are clustered in a manner that is independent of methylation state, but low-abundance receptors are significantly less clustered in the unmethylated state. They suggested that both increases in abundance and methylation may shift the equilibrium toward a clustered state, and that such an equilibrium could also regulate kinase activation.<sup>24</sup> Homma et al. reported that attractant ligand does not decrease the level of polar localization of a Tar-GFP construct in *E. coli*, but attractant does decrease the level of in vivo interdimer cross-linking of Tar.<sup>25</sup> By contrast, Lamanna et al. observed that attractant ligand decreases the size of polar clusters in both *E. coli* and *Bacillus subtilis*, when receptors are cross-linked with paraformaldehyde and then visualized with a fluorescent antibody.<sup>26</sup> Finally, Studdert and Parkinson reported that in vivo interdimer cross-linking of Tsr and Tar is independent of both ligand binding and methylation state.<sup>27</sup> Limitations of these studies include the inability of microscopy to distinguish clustering (oligomerization) of receptors from colocalization, and the inability of cross-linking studies to distinguish whether changes in the extent of cross-linking result from conformational changes or dissociation of receptors.

Two in vitro studies that correlated receptor concentration with changes in kinase activity are more suggestive that a clustering equilibrium may control the kinase. Lai et al.<sup>28</sup> varied the overexpression level of Tsr or Tar and isolated inner membrane vesicles that contained each receptor as a variable fraction of total membrane protein. The kinase activity per receptor increased linearly with receptor fraction, up to 50% of total membrane protein in these samples.<sup>28</sup> Besschetnova et al.<sup>29</sup> examined simpler, more defined samples of histidine-tagged cytoplasmic fragments of Tar<sub>4E</sub>, which were assembled

on the surface of liposomes with Ni-chelating lipids, along with CheA and CheW. These template-assembled receptor signaling arrays displayed a cooperative increase in the level of kinase activation as the two-dimensional receptor concentration on the vesicle increased. Moreover, receptor methylation activity was observed to *decrease* as the two-dimensional concentration (density) of receptors increased, in a manner consistent with the signaling equilibrium of Figure 1.<sup>29</sup> The results of these *in vitro* studies are consistent with a clustering equilibrium model in which high receptor concentrations favor the kinase-activating state, which would be a larger oligomeric (more clustered) state than the methylation-activating state. Such a model predicts that ligand binding would favor receptor dissociation into the kinase-inactivating state (less clustered) and thus ligand affinity (which was not measured in either study) would also vary with receptor concentration.

To test whether ligand-induced unclustering is an essential element of the mechanism of kinase regulation, we measured kinase activity and serine dose–response curves on purified *E. coli* Tsr reconstituted into liposomes over a range of two-dimensional concentrations of receptors. Our results indicate that the activity equilibrium does not involve a change in receptor oligomerization state. In combination with the previous template assembly results,<sup>29</sup> this indicates that the cytoplasmic domain of the kinase-off state has an expanded conformation.

## ■ EXPERIMENTAL PROCEDURES

**Purification of the Serine Receptor (Tsr).** Plasmids pJL41 and pJL31,<sup>30</sup> encoding Tsr<sub>4E</sub>Δ34His<sub>6</sub> and Tsr<sub>4Q</sub>Δ34His<sub>6</sub>, respectively (and constructed in a manner analogous to that of pJL21<sup>31</sup>), were used to express receptors with a C-terminal His tag to facilitate purification via nickel affinity chromatography. The receptors were expressed in HCB721, an *E. coli* strain that lacks CheR and CheB, so the receptor adaptation state was controlled genetically by the 4E and 4Q mutations. Cells were grown at 30 °C in LB containing 100 μg/mL ampicillin. Once an optical density between 0.4 and 0.6 at 600 nm had been reached, receptor expression was induced by the addition of 0.5 mM IPTG (final concentration), and then cells were grown for 3 h and harvested by centrifugation at 3750 rpm (Beckman Coulter Allegra 6R Tabletop Centrifuge; GH-3.8A swinging bucket rotor) for 15 min at 4 °C. Cell pellets were flash-frozen in liquid N<sub>2</sub> and stored at –80 °C until purification.

Cell pellets were thawed on ice and resuspended with 4 mL of resuspension buffer per gram of cells [50 mM Tris-HCl (pH 8), 300 mM NaCl, 10% glycerol, 1% (w/v) freshly prepared *n*-octyl β-D-glucopyranoside (OG) detergent, and 10 mM imidazole]. Lysozyme and PMSF (final concentrations of 0.15 mg/mL and 2 mM, respectively) were added, and cells were incubated on ice for 20 min. Sonication was performed with a Branson Ultrasonics sonicator, using a medium-sized tip, at a duty cycle of 35 and an output control of 3.5. The cell/lysozyme suspension was sonicated on ice for three 2 min intervals separated by cooling periods of 3 min. Cell debris was removed in a Beckman L80 ultracentrifuge at 28000 rpm (104000g; SW28 rotor) for 1 h at 4 °C. The supernatant, containing the OG-solubilized Tsr, was loaded onto a Ni-NTA column (5 mL HisTrap HP, GE Healthcare) pre-equilibrated with resuspension buffer for separation at 4 °C. The column was washed at 5 mL/min with 50 mL of resuspension buffer containing 50 mM imidazole, and Tsr was eluted at 3 mL/min with 30 mL of resuspension buffer containing 250 mM

imidazole. Fractions (3 mL) were collected and evaluated by SDS–PAGE. The Tsr-containing fractions were pooled, and EDTA was added to a final concentration of 1 mM to inhibit metalloproteases. Aliquots of the protein solution were flash-frozen in liquid nitrogen and stored at –80 °C.

**Reconstitution of Tsr into Lipid Vesicles.** *E. coli* polar lipid extract in chloroform (Avanti Polar Lipids) was dried to a thin film in a glass vial using N<sub>2</sub> gas. Reconstitution buffer [25 mM Tris-HCl, 25 mM NaCl, and 10% glycerol (pH 7.4)] was added to generate a 10 mg/mL suspension of lipid. The suspension was extruded 21 times through a 400 nm polycarbonate filter (Avanti Polar Lipids). Purified Tsr in 1% (w/v) OG was added to the lipid vesicles at various lipid:receptor ratios. More OG and PMSF were added to give final concentrations of 0.7% (w/v) and 2 mM, respectively. After a 1 h incubation at 25 °C, the lipid/detergent/receptor mixture was diluted 2-fold with detergent-free reconstitution buffer. Biobeads were added over time to the samples (stirred slowly with microstir bars) sequentially as follows. Aliquots of Biobeads, at a 2:1 (w/w) ratio of Biobeads to the initial amount of detergent, were added at 0, 30, and 60 min at 25 °C. Then at 90 min and 4 °C, an aliquot of Biobeads was added at a 15:1 ratio of Biobeads to the initial amount of detergent. Finally at 120 min, an aliquot of Biobeads was added at a 12:1 ratio of Biobeads to the initial amount of detergent for overnight incubation (approximately 16 h) at 4 °C. Using a pipet tip cut ~0.5 cm from the end of the tip, the resulting proteoliposome suspensions were removed from the settled Biobeads in each sample and centrifuged for 15–30 min at 14000 rpm (16000g). The pellets were resuspended in fresh, detergent-free reconstitution buffer. Samples were stable for ~1 month at 4 °C.

**Measurement of the Lipid:Receptor Ratio in Proteoliposomes.** The concentration of purified Tsr in detergent micelles was determined using a BCA protein assay (Pierce Protein Research). Such samples served as a standard for measurement of Tsr concentrations in proteoliposomes by SDS–PAGE, by comparing intensities of Tsr bands using ImageJ. The amount of lipid was determined using the molybdate assay for inorganic phosphate.<sup>32</sup> Aliquots from 0.01 to 0.10 mL of a 0.7 mM sodium phosphate (Na<sub>2</sub>HPO<sub>4</sub>) standard solution and test samples at different dilutions were placed in Pyrex 13 mm × 100 mm test tubes. A magnesium nitrate solution [30 μL of 10% Mg(NO<sub>3</sub>)<sub>2</sub>·6H<sub>2</sub>O in 95% ethanol] was added to each sample and then oven-dried overnight. The dried residue for each sample was ashed over an intense blue Bunsen flame in a fume hood until the evolution of brown NO<sub>2</sub> gas stopped. The tubes were cooled; 0.3 mL of 0.5 N HCl was added, and the tubes were capped with a marble and heated in a boiling water bath for 15 min. To minimize evaporation, a stream of air was used to cool the tops of the marbles. After the tubes were cooled, 0.7 mL of a solution consisting of 1 part ascorbic acid (10% w/v) and 6 parts ammonium molybdate stock solution [0.42% (w/v) ammonium molybdate tetrahydrate in 1 N H<sub>2</sub>SO<sub>4</sub>] was added to each tube (and to 0.3 mL of water for the blank). After incubation for 1 h at 37 °C, absorbance at 820 nm was measured. The phosphate concentrations in each test sample were found by comparison to a standard curve generated with Na<sub>2</sub>HPO<sub>4</sub>. The calculated [phosphate]/[Tsr] ratio provided the actual molar lipid:Tsr ratio in each sample.

**Ternary Complex Assembly and Binding Assays.** Ternary complexes of CheA, CheW, and Tsr proteoliposomes



were assembled at 25 °C overnight to test their kinase activities. High and low concentrations of CheA and CheW were used to assemble complexes with 16  $\mu$ M receptor in kinase buffer [75 mM Tris-HCl (pH 7.5), 100 mM KCl, 5 mM MgCl<sub>2</sub>, 2 mM TCEP, and 5% DMSO]. Low concentrations were 0.5  $\mu$ M CheA and 6  $\mu$ M CheW; high concentrations were 7  $\mu$ M CheA and 10  $\mu$ M CheW. The latter concentrations produced the greatest kinase activity with 16  $\mu$ M Tsr inner membrane preparations (A. Nelson, unpublished results). CheY was included in the overnight complex assembly for receptors assayed by [ $\gamma$ -<sup>32</sup>P]ATP incorporation.

After ternary complexes were assembled and incubated at 25 °C overnight, 30  $\mu$ L of the sample was sedimented in a Beckmann TLX tabletop ultracentrifuge at 60000 rpm (121000g) and 25 °C for 30 min. The supernatant was removed, and the remaining pellets, which contained the CheA bound to the receptors, were resuspended in 1 $\times$  kinase buffer to a final volume of 10  $\mu$ L to which was added 10  $\mu$ L of 2 $\times$  reducing gel loading buffer before boiling for 5 min. Using ImageJ, the intensities of CheA protein bands (on a 10% SDS gel) of the pellet gel samples were compared to a CheA standard series, allowing the determination of the concentration of bound CheA.

CheW binding was used to assess the accessibility of Tsr<sub>4E</sub> cytoplasmic domains in inner membrane preparations and reconstituted samples, relative to Tar<sub>4E</sub>CF assembled on liposomes, which were completely accessible.<sup>33</sup> Receptor (30  $\mu$ M) from each type of sample was incubated at 25 °C overnight with varying amounts of CheW in kinase buffer at 25 °C. Aliquots removed prior to sedimentation represented the total CheW in a sample, and aliquots removed from the supernatant after sedimentation at 25 °C (for 30 min at 121000g in a Beckman TLX tabletop ultracentrifuge with a TLA-120.2 rotor) represented unbound CheW. The total and unbound CheW samples were analyzed by SDS-PAGE on a 15% gel using ImageJ to compute the fraction of receptor-bound CheW as (total CheW – unbound CheW)/total CheW.

**Spectrophotometric ATPase Assay.** In this ATPase assay, regeneration of ATP is coupled to oxidation of NADH, which is monitored spectrophotometrically.<sup>34–36</sup> This assay was used only for optimization of reconstitution conditions (Figure 2), using a low lipid:receptor ratio of 100:1, because it suffers from excessive noise because of light scattering for high-lipid:receptor ratio proteoliposomes. Ternary complexes of 0.5  $\mu$ M CheA, 6  $\mu$ M CheW, and 16  $\mu$ M receptor in proteoliposomes were assembled in kinase buffer and incubated overnight at 25 °C. Following this incubation, 8  $\mu$ L of complex was diluted 25-fold into a final concentration of 50  $\mu$ M CheY, 4 units of lactose dehydrogenase/pyruvate kinase enzymes (Sigma Aldrich), 4 mM ATP, 4 mM phosphoenolpyruvate, and 0.25 mM NADH in kinase buffer. The decrease in absorbance (Abs) at 340 nm was monitored immediately. Specific activity (s<sup>-1</sup>) was calculated from the adjusted slope, the 6220 molar absorptivity of NADH, and the concentration of CheA in the reaction ( $2 \times 10^{-8}$  M), where adjusted slope = slope(CheY and complex) – slope(CheY and receptor only).

**[ $\gamma$ -<sup>32</sup>P]ATP Incorporation Assay.** To measure kinase activity by [ $\gamma$ -<sup>32</sup>P]ATP incorporation, ternary complexes of CheA, CheW, CheY, and receptor proteoliposomes were assembled and incubated overnight in kinase buffer at 25 °C. ATP fuel was prepared freshly in kinase buffer at a final concentration of 2 mM with 0.018 mCi of [ $\gamma$ -<sup>32</sup>P]ATP (10 mCi/mL, Perkin-Elmer) and kept at 25 °C; 0.5  $\mu$ L of kinase

buffer or serine was added to 4  $\mu$ L aliquots of assembled complexes and incubated at 25 °C for ~45 min. Phosphorylation reactions were initiated by addition of 4.5  $\mu$ L of the radioactive ATP, vortexed, and terminated after 15 s with the addition of 9  $\mu$ L of 2 $\times$  reducing SDS gel loading buffer. Three microliters of each sample (of 18  $\mu$ L total) was loaded on 16.5% SDS-PAGE gels. After drying, gels were exposed to a phosphorimager screen along with a dilution series of radioactive ATP spotted on filter paper and sealed in a plastic bag. The phosphor screen was scanned, and ImageQuant was used to estimate phosphate incorporation from the intensities of the <sup>32</sup>P-labeled CheY bands calibrated against the [ $\gamma$ -<sup>32</sup>P]ATP standards. The activity (s<sup>-1</sup>) of bound CheA was obtained by dividing the total activity per total CheA (s<sup>-1</sup>) by the fraction of bound CheA. Binding of CheA to the receptor was measured by SDS-PAGE using the most concentrated receptor samples (50:1 for Tsr<sub>4E</sub> and 60:1 for Tsr<sub>4Q</sub>) and applied across the series to calculate the activity per bound CheA.

## RESULTS

**Vesicle Reconstitution for Control of Receptor Concentration.** The strategy chosen for testing the effect of receptor concentration on its activation of CheA involves reconstitution of the purified intact receptor into vesicles at a range of lipid:receptor molar ratios for measurements of kinase activity and inhibition to test whether coupled ligand binding and receptor oligomerization equilibria control kinase activity (model shown in Figure 6).

Variables in the reconstitution of a membrane protein include the choice of lipid, detergent, method of detergent removal, and ratios of lipid to detergent and lipid to protein. The choice of both detergent [octyl  $\beta$ -D-glucopyranoside (OG)] and lipid (*E. coli* polar lipid extracts) was based on the fact that these were used in previous successful chemoreceptor solubilization and reconstitution studies.<sup>34,37</sup> Furthermore, the polar lipid extract contains phosphatidylethanolamine, phosphatidylglycerol, and cardiolipin at amounts similar to those found in the inner membrane of *E. coli*.<sup>38</sup> Purified Tsr was prepared by overexpression of constructs bearing a C-terminal truncation ( $\Delta$ 34) and an appended C-terminal His<sub>6</sub> tag in HCB721 cells, for purification by nickel-NTA affinity chromatography in a 1% (w/v) OG detergent. For optimization of reconstitution conditions, we tested a range of detergent:lipid ratios and several detergent removal methods, while maintaining the final lipid:receptor molar ratio at 100:1. Centrifugation followed by SDS gel electrophoresis of pellet and supernatant samples provided a rapid assay for determining the fraction of Tsr incorporated into the lipid vesicles upon detergent removal; ATP hydrolysis assays of receptors in the pellet fraction in ternary complexes with CheA and CheW provided a measure of receptor functionality.

The method developed by Rigaud and Levy<sup>39</sup> was used to optimize conditions for obtaining Tsr incorporated into vesicles with maximal kinase activity. A range of reconstitution conditions are prepared by adding various amounts of detergent to the preformed liposomes and measuring optical density to monitor solubilization as shown in Figure 2B. Light scattering remains high as OG detergent is titrated into the liposome suspension, producing detergent-destabilized liposomes. Light scattering then decreases as liposomes begin to solubilize into smaller lipid/detergent micelles, until it reaches a minimum OD close to zero when only lipid/detergent micelles

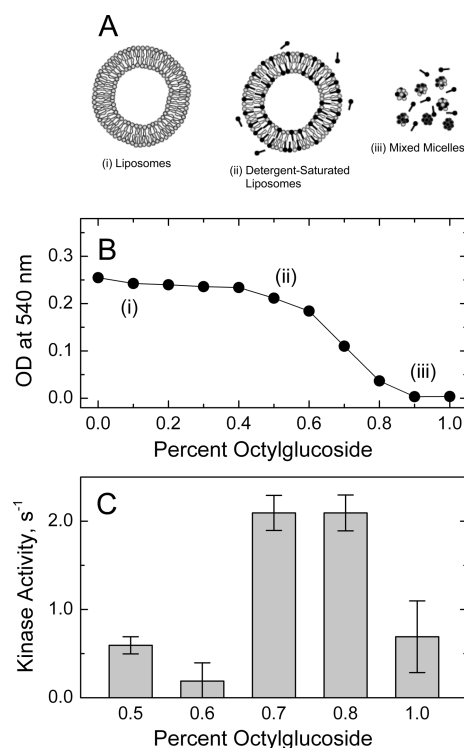


**Figure 2.** Optimal conditions for Tsr proteoliposome formation. (A and B) Conversion of phospholipid liposomes (2 mg of lipid/mL) into mixed micelles monitored by light scattering at 540 nm as a function of the OG [from 0.0 to 1.0% (w/v)] added to the liposomes. OG-solubilized affinity-purified Tsr was added to the solutions, and the OG was removed (as described in Experimental Procedures) to yield proteoliposomes. (C) Kinase activity of receptor–CheW–CheA complexes measured in the coupled ATPase assay using Tsr proteoliposomes prepared with different OG concentrations shown in panel B. Proteoliposomes prepared with either 0.7 or 0.8% OG (w/v) yielded the highest CheA activity.

are present. Purified Tsr was added to the various lipid/detergent mixtures, and the resulting membrane incorporation and kinase activation by the receptor were measured.

Initial experiments indicated that (1) the highest kinase activity is achieved with detergent concentrations near the middle of the liposome solubilization curve and (2) detergent removal with Biobeads can yield 100% incorporation of Tsr into the membrane fraction but reconstituted Tsr shows consistently higher levels of kinase activation when OG is diluted 2-fold before the addition of Biobeads (data not shown). Using this detergent removal method (2-fold dilution followed by Biobeads), reconstitutions were performed to find the optimal OG concentrations in the range of 0.5–1.0% by adding purified Tsr to the various lipid/detergent mixtures. As shown in Figure 2C, reconstitution using OG concentrations of 0.7–0.8% results in the greatest level of kinase activation; therefore, 0.7% OG (2 mg/mL lipids) was chosen for reconstitutions with a series of lipid:receptor ratios.

The challenges of quantitative studies of membrane proteins in proteoliposomes include limited access to the vesicle interior and light scattering by the vesicles. It is important to determine whether these accessibility and scattering issues are constant over the range of receptor concentrations to be compared in this study. We found that although light scattering was not a problem in the spectrophotometric assay at the higher receptor concentrations (lipid:receptor ratios of 50:1 to 300:1), it

resulted in unacceptably large errors for low-concentration samples.<sup>40</sup> Therefore, all kinase activation measurements reported below employed a <sup>32</sup>P incorporation assay in which light scattering was irrelevant.

The anticipated random incorporation of receptors into proteoliposomes during reconstitution would result in 50% of the intact receptors with their cytoplasmic domain exposed on the outside of the lipid vesicles. It is important to determine whether comparable amounts of cytoplasmic domains are accessible for complex formation and kinase activation across the range of samples that vary in receptor concentration. This was measured using CheW binding measurements on the low- and high-concentration extremes of the reconstitution sample series. Template-assembled cytoplasmic fragments (CF) of Tsr<sub>4E</sub> and inner membrane preparations (IMP) of Tsr<sub>4E</sub>, which are expected to have 100%<sup>33</sup> and ~90%<sup>41,42</sup> cytoplasmic accessibility, respectively, served as control samples for comparison with proteoliposomes containing reconstituted Tsr<sub>4E</sub>. As shown in Figure 3A, reconstituted samples with a

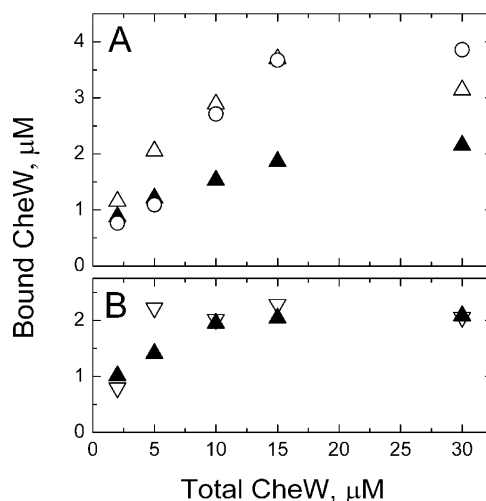


**Figure 3.** Receptor accessibility measured by CheW binding. (A) Cytoplasmic domains (30 μM), present either as CF assembled on liposomes (○) or as full-length Tsr in IMPs (Δ), served as positive controls for binding, which were assumed to have 100 and ~90% accessibility, respectively. Tsr<sub>4E</sub> (30 μM) in proteoliposomes (▲) bound approximately half the amount of CheW as the two controls, consistent with a random orientation of reconstituted receptors, with 50% of the cytoplasmic domains accessible for CheW binding. (B) Binding of CheW to 15 μM Tsr<sub>4E</sub> reconstituted at target lipid:protein ratios of 50:1 (▽) and 1000:1 (▲).

lipid:receptor ratio of 50:1 bound half the amount of CheW compared to the CF and IMP samples, as expected for random orientation with 50% cytoplasmic domains on the outside of the reconstituted proteoliposomes. Figure 3B demonstrates comparable CheW binding for the low (1000:1)- and high (50:1)-receptor concentration extremes of the Tsr<sub>4E</sub> proteoliposome series, demonstrating that the lipid:receptor ratio during the reconstitution does not alter the accessibility of the receptor cytoplasmic domain, which validates comparison of kinase activation across the sample series.

Finally, Ser inhibition of kinase activation requires that Ser have access to the vesicle interior to bind the periplasmic domains of those receptors with their exposed cytoplasmic domains on the vesicle exterior that can form complexes with CheA and CheW. As shown below, the series of reconstituted

Tsr<sub>4E</sub> proteoliposomes were nearly fully inhibited by Ser (~80% inhibition). This suggests that the proteoliposomes are leaky to small molecules. Such leakiness is consistent with the fact that lipid-only vesicles made via extrusion of *E. coli* polar lipids are leaky to Mn<sup>2+</sup>, based on broadening of 88% of the phosphorus NMR resonance of the lipid headgroups (M. Harris and D. Fowler, unpublished results). It is possible that such leakiness is not a property of the Tsr<sub>4Q</sub> proteoliposomes, because these receptors were not inhibited by Ser. However, in our hands, inner membrane preparations of Tsr<sub>4Q</sub> are also not inhibited by Ser. Because inner membrane samples are typically leaky because of the presence of porin impurities, this suggests some other cause of the locked-on state of Tsr<sub>4Q</sub>.

**Kinase Activation Is Independent of Receptor Concentration.** Proteoliposomes containing a range of intact Tsr concentrations were prepared using the optimized reconstitution protocol that combines OG-solubilized purified receptor with detergent-destabilized extruded vesicles (0.7% OG), followed by a 2-fold dilution and detergent removal with Biobeads. Different amounts of receptor were added to 2 mg/mL liposomes, with target lipid:receptor molar ratios ranging from 50:1 to 1000:1. Measurements of the protein and phosphate concentration in the resuspended proteoliposome samples were used to compute the actual lipid:receptor molar ratios, which ranged from 55:1 to 603:1. Ternary complexes of each of the proteoliposome samples were assembled so that they contained 16  $\mu$ M Tsr, 7  $\mu$ M CheA, and 10  $\mu$ M CheW, incubated at 25 °C overnight, and then subjected to <sup>32</sup>P incorporation assays of kinase activation and SDS–PAGE assays of CheA binding.

The data in Figure 4A and Table S1 of the Supporting Information demonstrate that kinase activity and inhibition by serine are independent of receptor concentration in proteoliposomes containing reconstituted Tsr<sub>4E</sub>. The absence of any effect of concentration on activity was observed at both high-CheA and -CheW concentration [16  $\mu$ M Tsr, 7  $\mu$ M CheA, and 10  $\mu$ M CheW (Figure 4A)] conditions under which a maximum in the total kinase signal was observed, and at lower CheA and CheW concentrations [16  $\mu$ M Tsr, 0.5  $\mu$ M CheA, and 6  $\mu$ M CheW (data not shown)]. As demonstrated in Figure 4A ( $\Delta$ ), the variations in activity among the samples are all within error, and there is no trend in activity with receptor concentration. Reconstituted Tsr<sub>4E</sub> proteoliposomes show similar inhibition (~80%) by serine at all receptor concentrations [Figure 4A ( $\blacktriangle$ ): the average kinase activity of 2.3 s<sup>-1</sup> decreases to 0.5 s<sup>-1</sup> per bound CheA in the presence of serine.

Activity assays on a similar series of proteoliposomes containing reconstituted Tsr<sub>4Q</sub> again demonstrate that kinase activation is independent of receptor concentration. The target and actual lipid:receptor ratios for both the Tsr<sub>4Q</sub> and Tsr<sub>4E</sub> reconstitution series (Tables S1 and S2 of the Supporting Information) are close at high receptor concentrations but diverge at low concentrations. Tsr<sub>4Q</sub> complexes were prepared under high-CheA and -CheW concentration conditions for kinase assays; the activity data are listed in Table S2 of the Supporting Information and plotted in Figure 4B. As observed for Tsr<sub>4E</sub>, there is no clear trend in kinase activation with Tsr<sub>4Q</sub> receptor concentration ( $\diamond$ ), and all activities are within a range similar to the variation between replicate measurements. The exception is the high-concentration receptor sample (~60:1 lipid:receptor ratio), which has a reproducibly low activity in the Tsr<sub>4Q</sub> series.

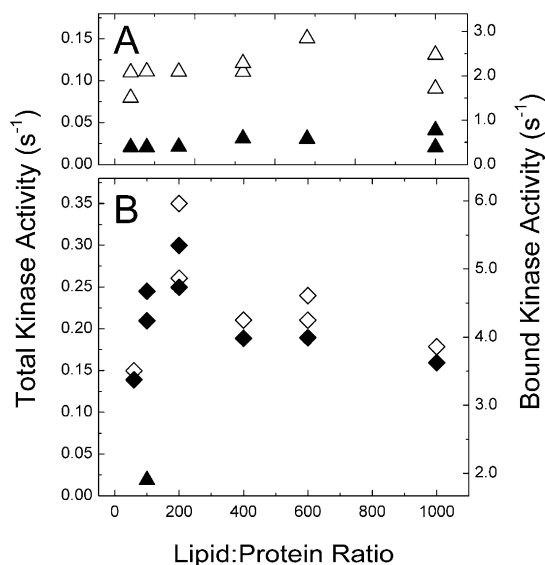


**Figure 4.** Kinase activity of receptor–CheW–CheA complexes as a function of the lipid:protein ratio in proteoliposomes. Receptor–CheW–CheA complex assembly conditions: 16  $\mu$ M receptor, 7  $\mu$ M CheA, and 10  $\mu$ M CheW incubated overnight at 25 °C. Kinase activities (<sup>32</sup>P incorporation assay) are scaled to the total amount of CheA added (7  $\mu$ M, left y-axis) and to the amount of CheA bound in the complex (right y-axis). (A) Kinase activities of Tsr<sub>4E</sub> proteoliposomes without serine ( $\Delta$ ) and with 10 mM serine ( $\blacktriangle$ ). (B) Kinase activities of Tsr<sub>4Q</sub> proteoliposomes without serine ( $\diamond$ ) and with 10 mM serine ( $\blacklozenge$ ). In contrast to the locked-on property of Tsr<sub>4Q</sub> proteoliposomes, a 100:1 4E sample included in the same series is inhibited 90% by 10 mM serine ( $\blacktriangle$ ).

Although kinase activation of Tsr<sub>4Q</sub> is comparable to that of Tsr<sub>4E</sub>, a surprising result is that none of the Tsr<sub>4Q</sub> proteoliposomes are inhibited by serine ( $\blacklozenge$ ). In contrast, a Tsr<sub>4E</sub> sample included with this series [Figure 4B ( $\blacktriangle$ )] is 90% inhibited by 10 mM Ser (see Table S2 of the Supporting Information). Additional activity measurements on the 100:1 samples demonstrated that even 400 mM Ser did not inhibit kinase activation by Tsr<sub>4Q</sub> proteoliposomes.<sup>40</sup> The lack of Ser inhibition of Tsr<sub>4Q</sub> might be related to the C-terminal deletion in our construct, because deletions of residues in the range of residues 502–515 of the Asp receptor have been shown to interfere with Asp inhibition of kinase activity.<sup>43</sup> However, our Tsr construct is intact through residue 517 and is capable of wild-type levels of kinase inhibition, at least for the Tsr<sub>2QE</sub><sup>31</sup> and Tsr<sub>4E</sub> (this study) methylation states.

**Ligand Inhibition of Kinase Is Independent of Receptor Concentration.** Measurements of ligand affinity can further test the clustering equilibrium model. If ligand binding turns off kinase activation by unclustering the receptor, the low-concentration conditions that favor the kinase-off state should yield receptors with higher ligand affinity. An indirect measure of ligand affinity via inhibition of kinase is ideal because it measures binding only to receptors in receptor–CheA–CheW complexes. Proteoliposomes containing Tsr<sub>4E</sub> reconstituted at high and low concentrations were titrated with serine to determine the concentration of serine at half-maximal kinase activity. The kinase assay results plotted in Figure 5 for target lipid:receptor molar ratios of 50:1 (black triangles) and 1000:1 (gray circles) demonstrate that the serine inhibition profile is not significantly different at the two concentration extremes. The titration data were fit to the Hill



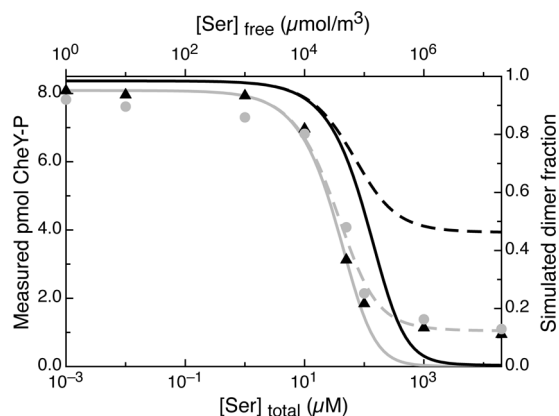


**Figure 5.** The apparent serine affinity ( $IC_{50}$ ) of  $Tsr_{4E}$  is independent of receptor concentration. Data are plotted using the left y-axis and bottom x-axis. Experimentally observed amounts of CheY- $^{32}P$  (picomoles in 3  $\mu$ L gel band) generated by receptor–CheW–CheA complexes containing  $Tsr_{4E}$  in proteoliposomes reconstituted at target lipid:receptor ratios of 50:1 ( $\blacktriangle$ ) and 1000:1 (gray circles) are plotted as a function of the total serine concentration. Error bars, representing the standard deviation of the CheY-P band intensities when one  $^{32}P$  reaction mixture was loaded twice on the gel, are smaller than the data symbols on the plot. Simulations were plotted using the right y-axis and top x-axis. The simulated dimer fraction for a simple ligand-induced dissociation model (Figure 6A, with  $K = 4 \times 10^{-4} \text{ m}^3/\mu\text{mol}$  and  $K_x = 10^5 \text{ m}^2/\mu\text{mol}$ ) is plotted as a function of free serine concentration. Gray lines represent simulations for the low-concentration receptor sample (RC1000,  $4 \times 10^{-3} \mu\text{mol}/\text{m}^2$ ), and black lines represent simulations for the high-concentration receptor sample (RC50,  $4 \times 10^{-2} \mu\text{mol}/\text{m}^2$ ). Dissociation constants for the model are chosen so that ligand binding causes complete inhibition (solid lines with  $K_1 = K_2 = 4 \times 10^{-7} \text{ m}^3/\mu\text{mol}$ ) or partial inhibition (dashed lines with  $K_1 = K_2 = 8 \times 10^{-6} \text{ m}^3/\mu\text{mol}$ ). For both cases, the model predicts a measurable change (gray to black) in the inhibition curve over the 10-fold change in receptor concentration tested. The data show no such change and thus refute the ligand-induced dissociation model.

**Table 1. Serine Binding Parameters for  $Tsr_{4E}$  Proteoliposomes<sup>a</sup>**

proteoliposome sample	50:1 (RC50)	1000:1 (RC1000)
[CheY-P] (pmol)	$8.05 \pm 0.04$	$7.30 \pm 0.06$
$\Delta$ [CheY-P] (pmol)	$-6.93 \pm 0.05$	$-6.20 \pm 0.06$
Hill coefficient ( $n_H$ )	$1.65 \pm 0.09$	$1.73 \pm 0.2$
[serine] $_{1/2}$ ( $\mu$ M)	$28 \pm 1$	$46 \pm 3$

<sup>a</sup>Titration data were fit using OriginPro (OriginLab) to a Hill function to obtain parameter values  $\pm$  the standard deviation of the fit:

$$[\text{CheY-P}] = [\text{CheY-P}]_0 + \Delta[\text{CheY-P}] \left( \frac{[\text{serine}]^{n_H}}{[\text{serine}]_{1/2}^{n_H} + [\text{serine}]^{n_H}} \right)$$

equation for a quantitative comparison; the resulting parameters are listed in Table 1. [Serine] $_{1/2}$ , the concentration at half-inhibition, shifts only slightly, from 28  $\mu$ M for the high-concentration receptor to 46  $\mu$ M for the low-concentration receptor. This is not a significant change and is in the opposite direction from the prediction of a ligand-modulated clustering equilibrium model: if ligand binding causes unclustering, low-concentration receptors would have a higher ligand affinity. Both samples also have similar Hill coefficients ( $n_H = 1.7$ ), indicating positive cooperativity similar to previous observations ( $n_H = 1.5$ ) for the  $Tsr_{4E}$  chemoreceptor.<sup>4</sup> The similarity of

ligand inhibition at high and low receptor concentrations indicates that ligand binding does not play a significant role in modulating the receptor association to control kinase activity.

The measured kinase activation properties of  $Tsr_{4E}$  at a range of concentrations were compared to a simplified model of a ligand-modulated dimerization equilibrium, based on the treatment by Wofsy et al.<sup>44</sup> and using pro Fit (Quantum Soft) to simulate the active dimer fraction of receptors. This model (Figure 6A) assumes that dimerization of some receptor unit (such as dimerization of two receptor trimers of dimers) is necessary to create the kinase-activating complex. Kinase activation is then proportional to the concentration of this active dimer fraction. Vertical reactions in the figure represent ligand binding, with association constants  $K$ ,  $K_1$ , and  $K_2$  (in three-dimensional units of cubic meters per micromole), and horizontal reactions represent receptor dimerization into the kinase-activating complex, with association constants  $K_x$ ,  $K_{x1}$ , and  $K_{x2}$  (in two-dimensional units of square meters per micromole). Note that only four of these six constants are independent, because  $K_{x1} = K_x K_1 / K$  and  $K_{x2} = K_x K_2 / K$ .

The high receptor activity in the absence of ligand at all tested concentrations [physiological range (see Discussion)] suggests that the ligand-free dissociated kinase-inactive receptor (top left in Figure 6A) does not occur under physiological conditions. As shown in Figure 6B, the concentration independence of kinase activation in the absence of Ser provides a lower limit for the receptor–receptor affinity in this kinase-activating unit: comparison of the measured activity (same data as plotted in Figure 4A) with simulated curves representing the predicted active dimer fraction for various values of  $K_x$  demonstrates that  $K_x \geq 10^4 \text{ m}^2/\mu\text{mol}$  if similar kinase activation is to be seen throughout the concentration series. A  $K_x$  value of  $10^5$  is used in simulations of the dimer fraction as a function of ligand concentration in Figure 5. In this model, ligand-induced dissociation of the active dimer occurs when the ligand affinity of the inactive “monomer” is greater than the ligand affinity of the active dimer ( $K > K_1$  and  $K_2$ ). Simulations can be used to predict the magnitude of the shift in [serine] $_{1/2}$  for the receptor inactivation transition, for comparison with the data. The simulated curves plotted in Figure 5 show that ligand binding would fully dissociate (and thus inactivate) the receptor dimer for both the high (solid black line)- and low (solid gray line)-receptor concentration extremes when  $K = 4 \times 10^{-4} \text{ m}^3/\mu\text{mol}$  and  $K_1 = K_2 = 4 \times 10^{-7} \text{ m}^3/\mu\text{mol}$ . Lower values of  $K_1$  and  $K_2$  (i.e.,  $4 \times 10^{-8} \text{ m}^3/\mu\text{mol}$ ) give superimposable curves, and higher values (i.e.,  $K_1 = K_2 = 8 \times 10^{-6} \text{ m}^3/\mu\text{mol}$ ) give incomplete inhibition (dashed lines). The  $K_x$  of  $1 \times 10^5$  was chosen for the simulations so the receptor would be close to fully dimerized and maximally active. For either complete (solid lines) or partial inhibition (dashed lines), the simulations predict a significant shift in [serine] $_{1/2}$  for the high- versus low-concentration receptor samples (Figure 5, black vs gray, respectively), which is not observed. These simulations demonstrate that the 10-fold change in receptor concentration in these two samples would have significantly shifted [serine] $_{1/2}$  for a ligand-induced receptor dissociation model, and thus, these data are sufficient to disprove this mechanism for ligand control of kinase activation.

## DISCUSSION

**Proteoliposomes Mimic Physiological Conditions To Test Clustering Mechanisms.** We have prepared proteoli-

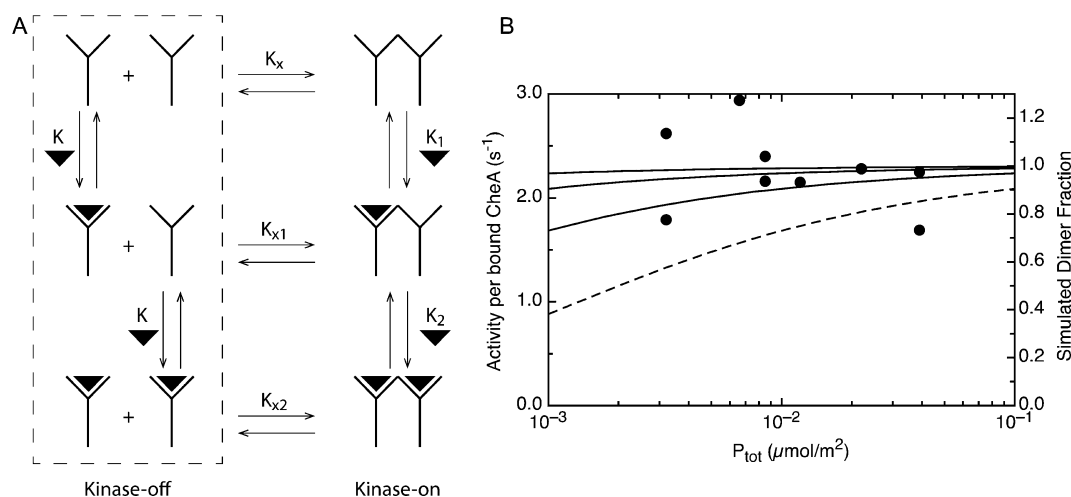


**Figure 6.** Simple ligand-modulated dimerization model for comparison with activity measurements. (A) In this model, the receptors must associate to form the kinase-activating unit, here represented as a “dimer” unit for the sake of simplicity (each “monomer” unit could correspond to a trimer of receptor dimers). Binding constants for ligand association (vertical reactions) are  $K$ ,  $K_1$ , and  $K_2$ . Binding constants for receptor association (horizontal reactions) are  $K_x$ ,  $K_{x1}$ , and  $K_{x2}$ . (B) The concentration independence of the Tsr<sub>4E</sub> receptor activity (●, left y-axis) in the absence of ligand can be compared to the calculated dimer fraction (right y-axis) for a range of values for  $K_x$ . The dashed line for  $K_x = 10^3 \text{ m}^2/\mu\text{mol}$  is incompatible with the data; the solid lines for  $K_x = 10^6$ ,  $10^5$ , and  $10^4 \text{ m}^2/\mu\text{mol}$  (from top to bottom, respectively) are compatible, providing a lower limit of  $K_x \geq 10^4 \text{ m}^2/\mu\text{mol}$ . Because the predicted ligand affinity shift with receptor concentration is not observed (Figure 5), the data suggest that the unclustered kinase-off receptor species in the dashed box (left side of panel A) do not occur under physiological conditions.

posomes containing purified bacterial chemotaxis receptors to control the receptor concentration and test the role of receptor oligomerization in ligand control of kinase activation. Our results demonstrate that both kinase activation and ligand affinity are independent of receptor concentration. Simulations indicate that we tested a sufficiently large change in receptor concentration to predict a measurable change in ligand affinity, thus demonstrating that modulation of an oligomerization or clustering equilibrium is not the means by which ligand binding controls kinase activation.

Proteoliposomes provide a good mimic of physiological conditions to test the role of receptor clustering in the mechanism of kinase activation. By incorporating the purified receptor into proteoliposomes, we avoided the variable amounts of protein impurities that result if receptor over-expression level is varied, to generate a series of samples that differ only in receptor concentration. As discussed below, the series of receptor proteoliposome samples spans a physiologically relevant range of lipid:protein ratios and exhibits kinase activities comparable to those reported for other *in vitro* receptor studies. The least physiological aspect of the proteoliposome sample is the mixed orientation of the receptors. The only purified receptor system that avoids this issue is the vesicle-templated CF,<sup>36</sup> but this system lacks the ligand-binding domain and thus cannot be used to investigate effects of receptor concentration on ligand affinity. Finally, proteoliposomes are advantageous over nanodisks<sup>20</sup> for a study of the effects of receptor clustering because the small nanodisks (~10 nm diameter) cannot accommodate physiologically relevant clusters that are observed in cells to extend over 200 nm.<sup>45</sup>

The Tsr proteoliposomes contain receptors in the concentration range expected for bacteria. An approximate physiological lipid:receptor molar ratio can be estimated as follows.<sup>46</sup> Because the receptors are found predominantly at the poles of the cells,<sup>3,24</sup> the area of the hemispherical cap is calculated as  $1/2(4\pi r^2) = 0.98 \mu\text{m}^2$ , for a cell diameter of 0.79  $\mu\text{m}$ . Using a

membrane surface area per lipid of 70  $\text{\AA}^2$ ,<sup>47</sup> the number of lipids at the cell poles =  $(0.98 \mu\text{m}^2 \text{ total area} / 7 \times 10^{-7} \mu\text{m}^2 \text{ area per lipid}) \times 2 \text{ membrane leaflets} \times 2 \text{ cell poles} = 5.6 \times 10^6$  lipids. This value for the number of polar lipids divided by reported estimates of 3600–41000 receptors per cell<sup>48</sup> yields a lipid:receptor molar ratio range of 1556:1 to 137:1. Super-resolution light microscopy measurements suggest that approximately two-thirds of Tar receptors localize to the poles,<sup>49</sup> which would increase the lipid:receptor molar ratio range at the poles to 2334:1 to 206:1. To calculate the effective lipid:receptor molar ratio in the Tsr proteoliposomes, the measured ratio ranging from 603:1 to 55:1 (see Table S1 of the Supporting Information) is corrected by a factor of 2 because only half of the receptors are oriented with the cytoplasmic domain accessible for assembly of complexes with CheA and CheW. Therefore, the experimental range from ~1200:1 to 100:1 is similar to the estimated physiological range from ~2300:1 to 200:1 at the cell poles.

It is important to note that an effective system for ligand control of receptor dissociation would likely position the coupled equilibrium for maximal ligand-induced change at physiological concentrations and densities. For example, simulations of the ligand-induced dissociation model described above can position the on–off transitions for the ligand-free and ligand-saturated receptor on either side of the physiological concentration range (transitions at  $P_{\text{tot}}$  values of 10<sup>-5</sup> and 1  $\mu\text{mol}/\text{m}^3$ , as shown in Figure S1 of the Supporting Information). Thus, throughout the physiological concentration range, the receptor would exhibit maximal (and constant) kinase activation and maximal inhibition by ligand binding. This suggests that the best way to detect such a coupled equilibrium is through its effects on ligand affinity (as shown in Figure 5) rather than effects on maximal activity, which are likely to be negligible.

Kinase activities achieved with the optimized reconstitution protocol compare favorably with previously reported activities. Activities are difficult to compare because of differences in



conditions for assembly of ternary complexes resulting in different amounts of bound CheA. Furthermore, the specific activity per total or per bound CheA is not always reported. The activity of Tsr<sub>4E</sub> proteoliposomes observed in this study ranges from  $\approx 2 \text{ s}^{-1}$  per total CheA (Figure 2, measured with the spectrophotometric assay with  $0.5 \mu\text{M}$  CheA) to  $\approx 0.1 \text{ s}^{-1}$  per total CheA  $\approx 2 \text{ s}^{-1}$  per bound CheA (Figure 4A, measured with the  $^{32}\text{P}$  incorporation assay with  $7 \mu\text{M}$  CheA). These values are similar to those obtained in the original reconstitution study of Ninfa et al. ( $3 \mu\text{M}$  ATP/min with  $0.2 \mu\text{M}$  CheA, equivalent to  $0.25 \text{ s}^{-1}$  per total CheA) for Tar<sub>2Q2E</sub>.<sup>34</sup> Similar activities in the range of  $0.15\text{--}1.5 \text{ s}^{-1}$  per total CheA have also been reported for native membrane vesicle preparations of Tsr<sub>2Q2E</sub><sup>4,28</sup> or Tar<sub>2Q2E</sub>.<sup>50</sup> Cytoplasmic fragment constructs (TarCF<sub>2Q2E</sub>) yield somewhat higher activities in the  $\approx 12 \text{ s}^{-1}$  range, when either bound to templating vesicles<sup>29</sup> or dimerized by leucine zippers.<sup>51</sup> Ligand binding curves for the proteoliposomes display cooperativity comparable to those of previous studies of receptors in native membrane vesicles, with Hill coefficients of  $\approx 1.5$  (ref 4) or  $1.7$  (this study) for Tsr<sub>4E</sub>, and  $\approx 1.8$  for Tsr<sub>2Q2E</sub><sup>28</sup> and Tar<sub>2Q2E</sub>.<sup>52</sup> However, values of the serine concentration at half-maximal inhibition vary widely, with  $35 \mu\text{M}$  for Tsr<sub>4E</sub> in proteoliposomes (this study) found between values previously observed for inner membrane vesicles: from  $\approx 0.1$  and  $5 \mu\text{M}$  for Tsr<sub>4E</sub> and Tsr<sub>2Q2E</sub>, respectively,<sup>4</sup> to  $\approx 260 \mu\text{M}$  for Tsr<sub>2Q2E</sub>.<sup>28</sup> With the exception of the locked-on state of Tsr<sub>4Q</sub> proteoliposomes observed in this study, which was not observed for Tsr<sub>4Q</sub> in inner membrane vesicles,<sup>4</sup> the proteoliposomes appear to have captured the physiological behavior of Tsr as well as previous in vitro preparations of intact chemotaxis receptors, while achieving control of receptor purity and concentration. In a different, in vivo, setting, Tar<sub>4E</sub> had a  $K_d$  of  $38 \mu\text{M}$  and an  $n_H$  of  $1.2$ .<sup>7</sup>

**Models for Ligand Control of Kinase Activation: Ligand Binding Expands the Receptor Structure without Changing the Number of Associated Receptors.** This study was motivated by a variety of results in the published literature that suggest a possible correlation between receptor clustering and receptor signaling state. Two studies in particular yielded data that strongly suggested that a high receptor concentration favors the kinase-activating state. Lai et al. prepared native membrane vesicles using a range of overexpression levels of intact receptors and found that the level of kinase activation increased linearly with the receptor fraction of total protein.<sup>28</sup> However, because the lipid and total protein content of the vesicles was not measured, it is not known how the receptor concentration varied among the samples. It is also possible that the receptor orientation in the isolated vesicles varied with receptor overexpression level. Native membrane vesicles isolated from cells with high levels of receptor overexpression are known to contain receptors oriented predominantly inside-out (accessible cytoplasmic domain). If a low level of overexpression yields a random orientation, then the increased activity observed with an increased level of overexpression could be due to an increasing fraction of receptors oriented with accessible kinase-binding cytoplasmic domains.

Besschetnova et al.<sup>29</sup> employed a simplified system with greater control of receptor concentration and orientation: purified receptor cytoplasmic fragments were bound via N-terminal His tags to vesicles bearing lipids with Ni-chelating headgroups. Thus, all receptors are bound to the outside of the

vesicle, accessible for kinase binding, and receptor concentration can be controlled precisely. A cooperative increase in kinase activity was observed with increasing receptor density on the vesicles, suggesting that the kinase-activating state is either (i) an oligomerized structure or (ii) a more compact structure, both of which would be favored by high receptor density. Results on intact receptors reconstituted into proteoliposomes now rule out model (i). Figure 7 summarizes this insight into

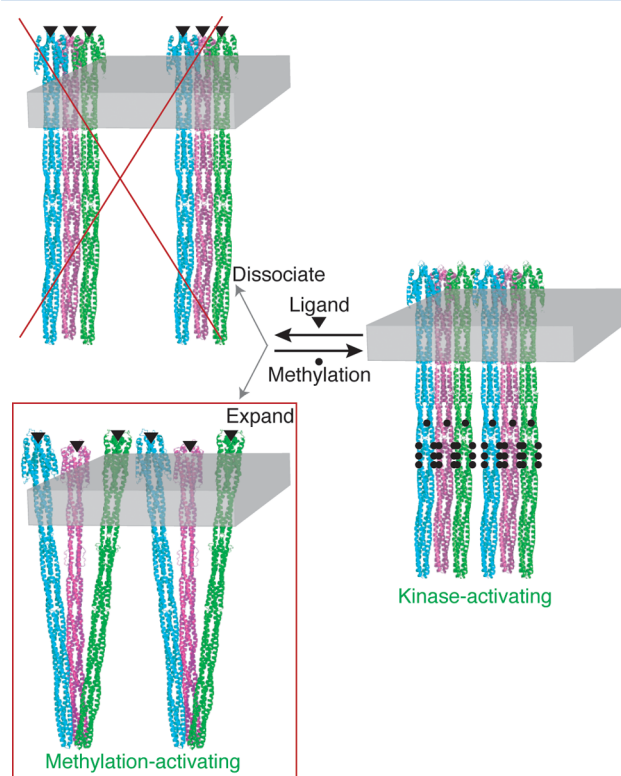


**Figure 7.** Model for kinase control. Six receptor dimers are shown associated as two trimers of dimers bound to a membrane slab of constant size (each dimer in a trimer is depicted in a different color). Cytoplasmic fragments assembled on vesicles are forced into the kinase-activating state by high density,<sup>29</sup> which would drive either an oligomerization or contraction of the receptor. The ligand-induced dissociation model is ruled out by the results reported above, the concentration independence of both kinase activity (Figure 4), and ligand affinity (Figure 5). Therefore, ligand binding induces an expanded receptor conformation.

the signaling mechanism: the kinase-activating state (right) forms the methylation-activating state either by dissociating (top) or by expanding (bottom). The dissociation model is eliminated by the current observations that receptor concentration does not alter kinase activity (Figure 4) or ligand affinity (Figure 5), which suggests that ligand binding induces an expanded receptor conformation.

Like chemoreceptors in cells, the intact Ser receptor (Tsr<sub>4E</sub>) adopts the kinase-activating state when reconstituted into proteoliposomes and is inhibited by Ser binding. In contrast, binding of the cytoplasmic fragment (TarCF<sub>4E</sub>) to membrane vesicles is not sufficient to create a kinase-activating state; high density is needed to drive it into the kinase-activating conformation. As noted previously, the density transition for TarCF<sub>4E</sub> mimics the two-state equilibrium shown in Figure 1: the density of the CF on vesicles, like ligand binding to intact receptors, causes inverse effects on methylation and kinase

activities.<sup>29</sup> Reconstitutions in this study all employed receptor densities lower than those used to drive the CF transition to the kinase-activating state (see the Supporting Information) and thus would not be expected to trap Tsr<sub>4E</sub> in a locked-on state, insensitive to inhibition by Ser. It is interesting that the 4Q receptor is found locked-on in both studies, with high kinase activity at both low density (vesicle-templated TarCF<sub>4Q</sub>) and high ligand concentration (Tsr<sub>4Q</sub> proteoliposomes).

Results of other studies have also suggested that the kinase-inactivating state of the receptor adopts an expanded conformation. Vaknin and Berg<sup>53</sup> showed that ligand binding to receptor-YFP constructs causes a 10% increase in the distance between the YFP fluorophores at the receptor C-termini. In a cryo-electron tomography study, Khursigara et al.<sup>54</sup> observed that ligand binding shifts the receptor population toward a conformation with an expanded HAMP domain. Both of these studies were performed on chemoreceptors in the absence of CheA and CheW. Our current results, interpreted in light of the template-assembled CF study,<sup>29</sup> suggest a similar conclusion for chemoreceptors in active complexes with CheA and CheW: attractant ligand binding to the receptor periplasmic domain turns off kinase activation by inducing an expanded receptor conformation that increases the membrane area occupied by each receptor cytoplasmic domain. In contrast to the results of Khursigara et al., this lateral expansion is not restricted to the HAMP domain, because it occurs in TarCF<sub>4E</sub> that lacks the HAMP domain. One possible model for the structural expansion is pictured in Figure 7: the expanded methylation-activating state, made by superimposing intact receptor models onto the trimer-of-dimers crystal structure of the cytoplasmic domain (Protein Data Bank entry 1qu7<sup>15</sup>), consists of tilted receptors that touch at their cytoplasmic tips, consistent with in vivo cross-linking results of Parkinson and co-workers that suggest such contacts occur in bacteria.<sup>27</sup> The contracted kinase-activating state, pictured as a parallel bundle of receptors, lacks the trimer-of-dimers contact at the tip, consistent with NMR measurements on the kinase-activating state.<sup>55</sup>

Further insight into the magnitude of the receptor expansion can be drawn from a recent electron cryotomography study of chemoreceptor arrays in *Caulobacter crescentus*. Briegel et al. showed that indistinguishable  $\approx 12$  nm hexagonal arrays are observed in the presence and absence of a galactose attractant.<sup>56</sup> Thus, the attractant does not dissociate the hexagonal arrays in *C. crescentus*, consistent with our in vitro demonstration that the attractant does not inhibit CheA kinase by dissociating *E. coli* chemoreceptors. Assuming *E. coli* and *C. crescentus* chemoreceptors operate similarly, the magnitude of the attractant-induced expansion of the cytoplasmic domain is below the detection limit of the published electron cryotomography study. Our work may also suggest that the overall expansion of the intact receptor is small, because we did not observe any change in ligand affinity with changes in receptor concentration and density in proteoliposomes.

In summary, we have demonstrated that the kinase activation and ligand affinity of bacterial chemoreceptors are independent of concentration, which provides insight into both the role of clustering and the mechanism of transmembrane signaling. Clustering changes may play a role in tuning the sensitivity of the receptor to the conditions of the cell: according to a recent study, *E. coli* grown under different environmental conditions (minimal vs rich media) exhibited differences in both the receptor arrays (density and/or order) and the sensitivity

(steepness) of the chemotaxis response curve.<sup>9</sup> The observed change in the response curve is not likely to be due to changes in overall receptor density, because our in vitro data demonstrate that changes in receptor density do not alter the cooperativity of the receptor. With regard to the transmembrane signaling mechanism, we have shown that clustering changes are not involved in the primary signal, ligand inhibition of the kinase. The primary signal occurs when ligand binding to the receptor induces a conformational change without changing the number of associated receptors in the signaling complex. This conformational change expands the lateral area of the membrane occupied by the receptor cytoplasmic domain. Further studies are needed to establish the structural details of the ligand-induced expansion of the cytoplasmic domain, how it is coupled via the HAMP domain to the ligand-induced piston that has been shown to occur in the periplasmic and transmembrane domains,<sup>57</sup> and how it inhibits the kinase activity of the associated CheA.

## ■ ASSOCIATED CONTENT

### ● Supporting Information

Comparison of receptor density in proteoliposomes (this study) and vesicle-templated CF<sup>29</sup> and Tables S1 and S2 listing kinase activities of proteoliposomes. This material is available free of charge via the Internet at <http://pubs.acs.org>.

## ■ AUTHOR INFORMATION

### Corresponding Author

\*Telephone: (413) 545-0827 (L.K.T.) or (413) 545-0464 (R.M.W.). Fax: (413) 545-4490. E-mail: [thompson@chem.umass.edu](mailto:thompson@chem.umass.edu) (L.K.T.) or [rmweis@chem.umass.edu](mailto:rmweis@chem.umass.edu) (R.M.W.).

### Funding

This research was supported by U.S. Public Health Service Grants GM47601 to L.K.T. and GM085288 to L.K.T. and R.M.W. and also in part by the U.S. Army Research Office under Grant 54635CH and a Faculty Research Grant from the University of Massachusetts, Amherst. F.C.S. was partially supported by a fellowship from the University of Massachusetts as part of the Chemistry-Biology Interface Training Program (National Research Service Award T32 GM08515).

### Notes

The authors declare no competing financial interest.

## ■ ACKNOWLEDGMENTS

We thank Jiayin Li for construction of plasmids pJL31 and pJL41, Abdalín Asinas for help with the initial activity assays, Seena Koshy for proteins used in some kinase assays, Dan Fowler and Michael Harris for NMR measurements of vesicle leakiness, and Adam Nelson for measurement of CheA and CheW levels that maximize kinase activity for inner membrane preparations.

## ■ ABBREVIATIONS

CF, aspartate receptor cytoplasmic fragment; DMSO, dimethyl sulfoxide; EDTA, ethylenediaminetetraacetic acid; EGF, epidermal growth factor; GFP, green fluorescent protein; HAMP, histidine kinases, adenyl cyclases, methyl-accepting proteins, and phosphatases; IMP, inner membrane preparation of overexpressed receptors in native membrane vesicles; IPTG, isopropyl  $\beta$ -D-1-thiogalactopyranoside; LB, Luria-Bertani; OD, optical density; OG, *n*-octyl  $\beta$ -D-glucopyranoside; PMSF, phenylmethanesulfonyl fluoride; RC, reconstituted proteolipo-

some; SDS–PAGE, sodium dodecyl sulfate–polyacrylamide gel electrophoresis; Tar, aspartate receptor; Tap, dipeptide receptor; TCEP, tris(2-carboxyethyl)phosphine; Trg, ribose/galactose receptor; Tsr, serine receptor; YFP, yellow fluorescent protein.

## REFERENCES

- (1) Wuichet, K., and Zhulin, I. B. (2010) Origins and diversification of a complex signal transduction system in prokaryotes. *Sci. Signaling*, 3.
- (2) Hazelbauer, G. L., and Lai, W. C. (2010) Bacterial chemoreceptors: Providing enhanced features to two-component signaling. *Curr. Opin. Microbiol.* 13, 124–132.
- (3) Maddock, J. R., and Shapiro, L. (1993) Polar location of the chemoreceptor complex in the *Escherichia coli* cell. *Science* 259, 1717–1723.
- (4) Li, G., and Weis, R. M. (2000) Covalent modification regulates ligand binding to receptor complexes in the chemosensory system of *Escherichia coli*. *Cell* 100, 357–365.
- (5) Li, M., and Hazelbauer, G. L. (2005) Adaptational assistance in clusters of bacterial chemoreceptors. *Mol. Microbiol.* 56, 1617–1626.
- (6) Duke, T. A., and Bray, D. (1999) Heightened sensitivity of a lattice of membrane receptors. *Proc. Natl. Acad. Sci. U.S.A.* 96, 10104–10108.
- (7) Sourjik, V., and Berg, H. C. (2002) Receptor sensitivity in bacterial chemotaxis. *Proc. Natl. Acad. Sci. U.S.A.* 99, 123–127.
- (8) Sourjik, V., and Berg, H. C. (2004) Functional interactions between receptors in bacterial chemotaxis. *Nature* 428, 437–441.
- (9) Khursigara, C. M., Lan, G., Neumann, S., Wu, X., Ravindran, S., Borgnia, M. J., Sourjik, V., Milne, J., Tu, Y., and Subramaniam, S. (2011) Lateral density of receptor arrays in the membrane plane influences sensitivity of the *E. coli* chemotaxis response. *EMBO J.* 30, 1719–1729.
- (10) Heldin, C. H. (1995) Dimerization of cell surface receptors in signal transduction. *Cell* 80, 213–223.
- (11) Weiss, A., and Schlessinger, J. (1998) Switching signals on or off by receptor dimerization. *Cell* 94, 277–280.
- (12) Falke, J. J., Bass, R. B., Butler, S. L., Chervitz, S. A., and Danielson, M. A. (1997) The two-component signaling pathway of bacterial chemotaxis: A molecular view of signal transduction by receptors, kinases, and adaptation enzymes. *Annu. Rev. Cell Dev. Biol.* 13, 457–512.
- (13) Yeh, J. I., Biemann, H. P., Pandit, J., Koshland, D. E., and Kim, S. H. (1993) The three-dimensional structure of the ligand-binding domain of a wild-type bacterial chemotaxis receptor. Structural comparison to the cross-linked mutant forms and conformational changes upon ligand binding. *J. Biol. Chem.* 268, 9787–9792.
- (14) Hulko, M., Berndt, F., Gruber, M., Linder, J. U., Truffault, V., Schultz, A., Martin, J., Schultz, J. E., Lupas, A. N., and Coles, M. (2006) The HAMP domain structure implies helix rotation in transmembrane signaling. *Cell* 126, 929–940.
- (15) Kim, K. K., Yokota, H., and Kim, S. H. (1999) Four-helical-bundle structure of the cytoplasmic domain of a serine chemotaxis receptor. *Nature* 400, 787–792.
- (16) Wu, J., Li, J., Li, G., Long, D. G., and Weis, R. M. (1996) The receptor binding site for the methyltransferase of bacterial chemotaxis is distinct from the sites of methylation. *Biochemistry* 35, 4984–4993.
- (17) Barnakov, A. N., Barnakova, L. A., and Hazelbauer, G. L. (1999) Efficient adaptational demethylation of chemoreceptors requires the same enzyme-docking site as efficient methylation. *Proc. Natl. Acad. Sci. U.S.A.* 96, 10667–10672.
- (18) Dunten, P., and Koshland, D. E., Jr. (1991) Tuning the responsiveness of a sensory receptor via covalent modification. *J. Biol. Chem.* 266, 1491–1496.
- (19) Briegel, A., Ortega, D. R., Tocheva, E. I., Wuichet, K., Li, Z., Chen, S., Muller, A., Iancu, C. V., Murphy, G. E., Dobro, M. J., Zhulin, I. B., and Jensen, G. J. (2009) Universal architecture of bacterial chemoreceptor arrays. *Proc. Natl. Acad. Sci. U.S.A.* 106, 17181–17186.
- (20) Li, M., and Hazelbauer, G. L. (2011) Core unit of chemotaxis signaling complexes. *Proc. Natl. Acad. Sci. U.S.A.* 108, 9390–9395.
- (21) Briegel, A., Li, X., Bilwes, A. M., Hughes, K. T., Jensen, G. J., and Crane, B. R. (2012) Bacterial chemoreceptor arrays are hexagonally packed trimers of receptor dimers networked by rings of kinase and coupling proteins. *Proc. Natl. Acad. Sci. U.S.A.* 109, 3766–3771.
- (22) Liu, J., Hu, B., Morado, D. R., Jani, S., Manson, M. D., and Margolin, W. (2012) Molecular architecture of chemoreceptor arrays revealed by cryoelectron tomography of *Escherichia coli* minicells. *Proc. Natl. Acad. Sci. U.S.A.* 109, E1481–E1488.
- (23) Liberman, L., Berg, H. C., and Sourjik, V. (2004) Effect of chemoreceptor modification on assembly and activity of the receptor-kinase complex in *Escherichia coli*. *J. Bacteriol.* 186, 6643–6646.
- (24) Lybarger, S. R., Nair, U., Lilly, A. A., Hazelbauer, G. L., and Maddock, J. R. (2005) Clustering requires modified methyl-accepting sites in low-abundance but not high-abundance chemoreceptors of *Escherichia coli*. *Mol. Microbiol.* 56, 1078–1086.
- (25) Homma, M., Shiomu, D., and Kawagishi, I. (2004) Attractant binding alters arrangement of chemoreceptor dimers within its cluster at a cell pole. *Proc. Natl. Acad. Sci. U.S.A.* 101, 3462–3467.
- (26) Lamanna, A. C., Ordal, G. W., and Kiessling, L. L. (2005) Large increases in attractant concentration disrupt the polar localization of bacterial chemoreceptors. *Mol. Microbiol.* 57, 774–785.
- (27) Studdert, C. A., and Parkinson, J. S. (2004) Crosslinking snapshots of bacterial chemoreceptor squads. *Proc. Natl. Acad. Sci. U.S.A.* 101, 2117–2122.
- (28) Lai, R. Z., Manson, J. M., Bormans, A. F., Draheim, R. R., Nguyen, N. T., and Manson, M. D. (2005) Cooperative signaling among bacterial chemoreceptors. *Biochemistry* 44, 14298–14307.
- (29) Besschetnova, T. Y., Montefusco, D. J., Asinas, A. E., Shrout, A. L., Antommattei, F. M., and Weis, R. M. (2008) Receptor density balances signal stimulation and attenuation in membrane-assembled complexes of bacterial chemotaxis signaling proteins. *Proc. Natl. Acad. Sci. U.S.A.* 105, 12289–12294.
- (30) Li, J. (1996) Seeking the primary sense: A biochemical and biophysical study of the signaling mechanism of bacterial chemotaxis. Ph.D. Thesis, University of Massachusetts, Amherst, MA.
- (31) Li, J., Li, G., and Weis, R. M. (1997) The serine chemoreceptor from *Escherichia coli* is methylated through an inter-dimer process. *Biochemistry* 36, 11851–11857.
- (32) Ames, B. N. (1966) Assay of inorganic phosphate, total phosphate and phosphatases. *Methods Enzymol.* 8, 115–118.
- (33) Asinas, A. E., and Weis, R. M. (2006) Competitive and cooperative interactions in receptor signaling complexes. *J. Biol. Chem.* 281, 30512–30523.
- (34) Ninfa, E. G., Stock, A., Mowbray, S., and Stock, J. (1991) Reconstitution of the bacterial chemotaxis signal transduction system from purified components. *J. Biol. Chem.* 266, 9764–9770.
- (35) Norby, J. G. (1988) Coupled assay of Na<sup>+</sup>/K<sup>+</sup>-ATPase activity. *Methods Enzymol.* 156, 116–119.
- (36) Shrout, A. L., Montefusco, D. J., and Weis, R. M. (2003) Template-directed assembly of receptor signaling complexes. *Biochemistry* 42, 13379–13385.
- (37) Bogonez, E., and Koshland, D. E., Jr. (1985) Solubilization of a vectorial transmembrane receptor in functional form: Aspartate receptor of chemotaxis. *Proc. Natl. Acad. Sci. U.S.A.* 82, 4891–4895.
- (38) Morein, S., Andersson, A., Rilfors, L., and Lindblom, G. (1996) Wild-type *Escherichia coli* cells regulate the membrane lipid composition in a “window” between gel and non-lamellar structures. *J. Biol. Chem.* 271, 6801–6809.
- (39) Rigaud, J. L., and Levy, D. (2003) Reconstitution of membrane proteins into liposomes. *Methods Enzymol.* 372, 65–86.
- (40) Consolacion, F. C. (2011) Clustering independence of ligand affinity and kinase activity of reconstituted bacterial chemoreceptors: Insight into signaling mechanisms. Ph.D. Thesis, University of Massachusetts, Amherst, MA.
- (41) Gegner, J. A., Graham, D. R., Roth, A. F., and Dahlquist, F. W. (1992) Assembly of an MCP receptor, CheW, and kinase CheA



complex in the bacterial chemotaxis signal transduction pathway. *Cell* 70, 975–982.

(42) Levit, M. N., Grebe, T. W., and Stock, J. B. (2002) Organization of the receptor-kinase signaling array that regulates *Escherichia coli* chemotaxis. *J. Biol. Chem.* 277, 36748–36754.

(43) Lai, R. Z., Bormans, A. F., Draheim, R. R., Wright, G. A., and Manson, M. D. (2008) The region preceding the C-terminal NWETF pentapeptide modulates baseline activity and aspartate inhibition of *Escherichia coli* Tar. *Biochemistry* 47, 13287–13295.

(44) Wofsy, C., Goldstein, B., Lund, K., and Wiley, H. S. (1992) Implications of epidermal growth factor (EGF) induced EGF receptor aggregation. *Biophys. J.* 63, 98–110.

(45) Zhang, P., Khursigara, C. M., Hartnell, L. M., and Subramaniam, S. (2007) Direct visualization of *Escherichia coli* chemotaxis receptor arrays using cryo-electron microscopy. *Proc. Natl. Acad. Sci. U.S.A.* 104, 3777–3781.

(46) Asinas, A. E. (2007) Protein interactions and kinase regulation in template-assembled complexes of chemotaxis receptor fragments. Ph.D. Thesis, University of Massachusetts, Amherst, MA.

(47) Nagle, J. F., and Tristram-Nagle, S. (2000) Structure of lipid bilayers. *Biochim. Biophys. Acta* 1469, 159–195.

(48) Li, M., and Hazelbauer, G. L. (2004) Cellular stoichiometry of the components of the chemotaxis signaling complex. *J. Bacteriol.* 186, 3687–3694.

(49) Greenfield, D., McEvoy, A. L., Shroff, H., Crooks, G. E., Wingreen, N. S., Betzig, E., and Liphardt, J. (2009) Self-organization of the *Escherichia coli* chemotaxis network imaged with super-resolution light microscopy. *PLoS Biol.* 7, e1000137.

(50) Borkovich, K. A., Kaplan, N., Hess, J. F., and Simon, M. I. (1989) Transmembrane signal transduction in bacterial chemotaxis involves ligand-dependent activation of phosphate group transfer. *Proc. Natl. Acad. Sci. U.S.A.* 86, 1208–1212.

(51) Liu, Y., Levit, M., Lurz, R., Surette, M. G., and Stock, J. B. (1997) Receptor-mediated protein kinase activation and the mechanism of transmembrane signaling in bacterial chemotaxis. *EMBO J.* 16, 7231–7240.

(52) Bornhorst, J. A., and Falke, J. J. (2000) Attractant regulation of the aspartate receptor-kinase complex: Limited cooperative interactions between receptors and effects of the receptor modification state. *Biochemistry* 39, 9486–9493.

(53) Vaknin, A., and Berg, H. C. (2007) Physical responses of bacterial chemoreceptors. *J. Mol. Biol.* 366, 1416–1423.

(54) Khursigara, C. M., Wu, X., Zhang, P., Lefman, J., and Subramaniam, S. (2008) Role of HAMP domains in chemotaxis signaling by bacterial chemoreceptors. *Proc. Natl. Acad. Sci. U.S.A.* 105, 16555–16560.

(55) Fowler, D. J., Weis, R. M., and Thompson, L. K. (2010) Kinase-active signaling complexes of bacterial chemoreceptors do not contain proposed receptor-receptor contacts observed in crystal structures. *Biochemistry* 49, 1425–1434.

(56) Briegel, A., Beeby, M., Thanbichler, M., and Jensen, G. J. (2011) Activated chemoreceptor arrays remain intact and hexagonally packed. *Mol. Microbiol.* 82, 748–757.

(57) Falke, J. J., and Hazelbauer, G. L. (2001) Transmembrane signaling in bacterial chemoreceptors. *Trends Biochem. Sci.* 26, 257–265.